Supporting information

Ca^{2+} determines the entropy changes associated with the formation of transition states during water oxidation by Photosystem II.

Fabrice Rappaport,[†] Naoko Ishida,[‡] Miwa Sugiura,[⊥] and Alain Boussac[‡]

[†]IBPC, UMR 7141 CNRS and Université Pierre et Marie Curie, 13 rue Pierre et Marie Curie, 75005 Paris, France.

[‡]iBiTec-S, CNRS URA 2096, CEA Saclay, 91191 Gif-sur-Yvette, France.

[⊥]Cell-Free Science and Technology Research Center, Ehime University, Bunkyo-cho, Matsuyama Ehime, 790-8577, Japan.

CORRESPONDING AUTHORS Fabrice.rappaport@ibpc.fr, Alain.boussac@cea.fr

-Figure S1 shows that the cw EPR spectra recorded on the D2 Y60F Ca-PSII and D2 Y160F Sr-PSII used in this study are very similar if not identical to those already published (Low temperature photochemistry in Photosystem II from *Thermosynechococcus elongatus* induced by visible and near-infrared light.Boussac, A., Sugiura, M., Lai, T.-L. and Rutherford, A. W. (2008) *Phil. Trans. R. Soc.* 363, 1203-1210.)

-Figure S2 shows that the frequency domain of the light-*minus*-dark ESEEM data induced by the NIR illumination in the S$_3$-state in both D2 Y60F Ca-PSII and D2 Y160F Sr-PSII exhibit only peaks around the Larmor frequency of proton.

-Figure S3 compares the power spectra after Fourier transform of light-*minus*-dark ESEEM data induced by a NIR illumination in the S$_3$-state in both D2 Y60F Ca-PSII and D2 Y160F Sr-PSII. The ESEEM data were normalized to the same amplitude before the Fourier transform. This figure shows that the couplings originating from proton(s) are much less pronounced in D2 Y160F Sr-PSII than in D2 Y60F Ca-PSII.

-Figures S4 allows us to compare, as an example, the oscillating pattern at 292 nm and 440-426 nm in WT* Sr-PSII at 19°C.

-Figure S5 allows us to compare the oscillating pattern at 292 nm in WT* Sr-PSII at 5°C, 19°C and 40°C. The damping is only very slightly enhanced at 5°C and 40°C.

-Figure S6 shows that the temperature affects similarly the damping in WT* Sr-PSII and WT* Ca-PSII.

Figure S1:

Figure S1 shows the cw-EPR spectra recorded in D2-Y160F Ca-PSII (Panel A) and D2-Y160F Sr-PSII (Panel B). Spectra were recorded in the S_3-state (black spectra) and after a further NIR illumination at 820 nm in the EPR cavity at 4 K (red spectra). Shown in blue are the (S_3+NIR)-minus-(S_3) difference spectra.
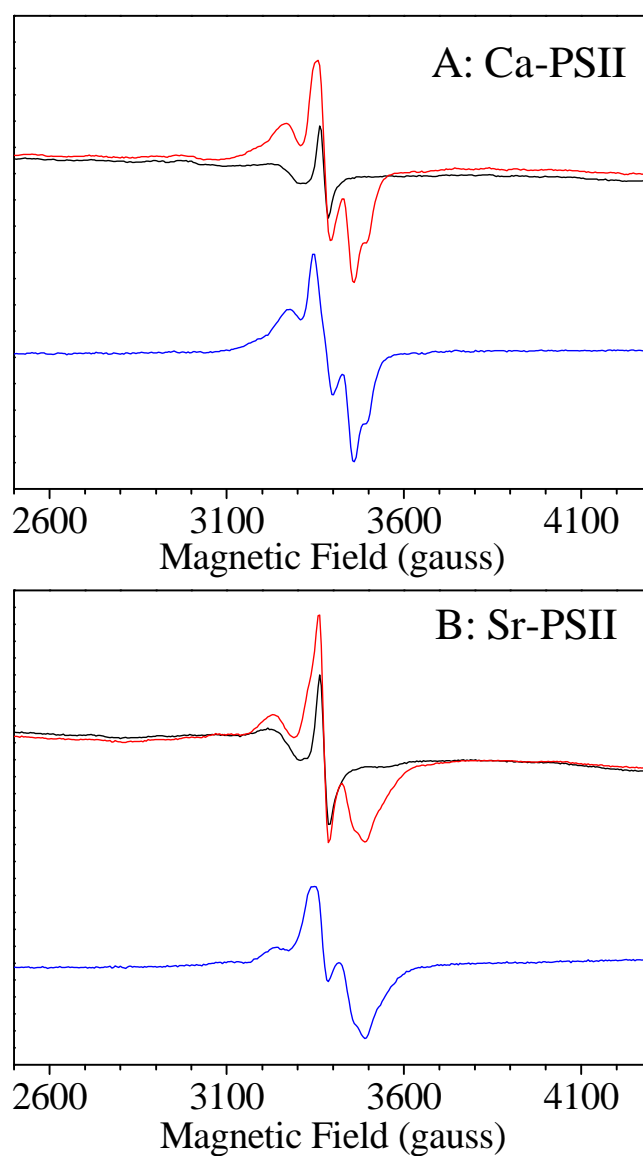
Instrument settings: modulation amplitude, 10 G; microwave power, 20 mW; microwave frequency, 9.4 GHz; modulation frequency, 100 kHz and temperature, 4.2 K. The chlorophyll concentration was 1.1 mg/ml.

Figure S2:

Pulse-EPR measurements in D2 Y160F Ca-PSII (Panel A) and D2 Y160F Sr-PSII (Panel B). The spectra are the power spectra of the Fourier transform of the ESEEM data recorded in the S_3-state (black spectra). The blue spectra are the power spectra of the Fourier transform of the light-*minus*-dark difference ESEEM spectra induced by NIR illumination at 820 nm at 4.2 K in the EPR cavity. ESEEM spectra were measured at 3484 gauss and resulted from a three-pulse sequence $\pi/2$-τ-$\pi/2$-T-$\pi/2$-echo with $\tau = 168$ ns and Tmin = 64 ns. Temperature = 4.2 K; microwave frequency, 9.7 GHz. Shot repetition time = 8 ms. The $\pi/2$ pulses duration was 16 ns. For the ESEEM, 800 points were recorded and T was incremented by 8 ns steps from its initial value (64 ns). Fourier transform of the time domain data was done after: (1) subtraction of a background double exponential function, (2) zero-filling to 1024 points, (3) dead-time reconstruction by simulating peaks in the frequency domain followed by a back Fourier transform to fill the missing data in the dead time, and (4) Fourier transform of the full data (experimental + reconstructed dead time).
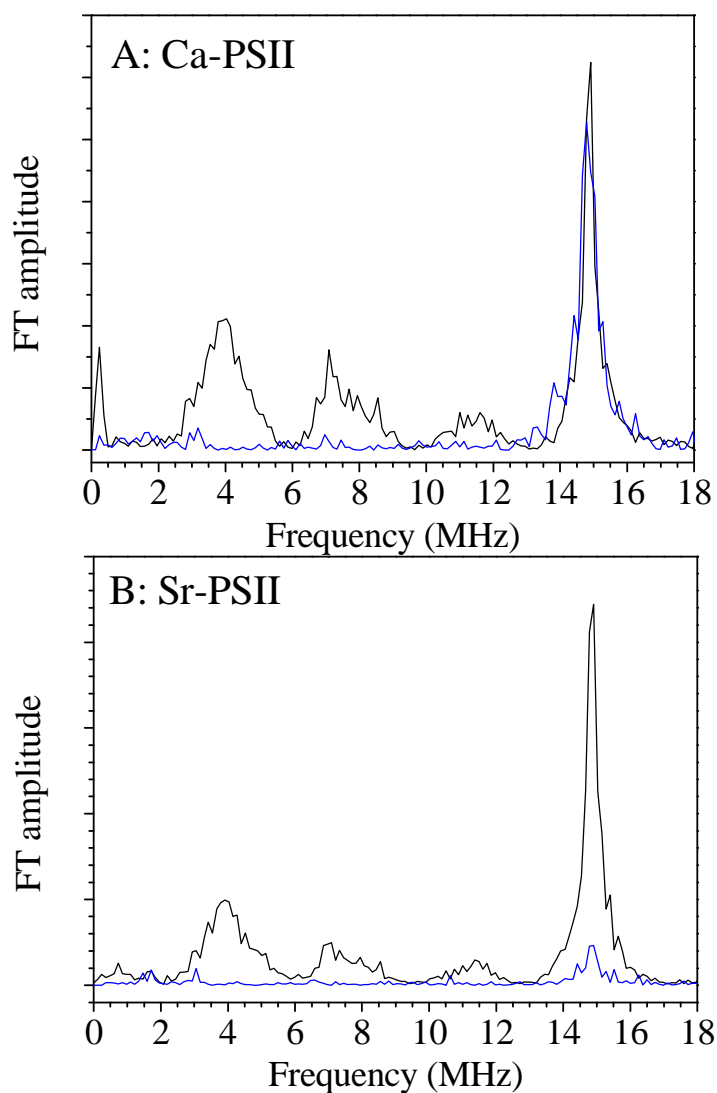
Figure S3:

Pulse-EPR measurements in D2 Y160F Ca-PSII (black spectrum) and D2 Y160F Sr-PSII (Red spectrum). Power spectra of the light-*minus*-dark difference ESEEM spectra Fourier transform shown in Figure S2. Before Fourier transform, the ESEEM data in Ca-PSII and Sr-PSII were normalized to the same amplitude.
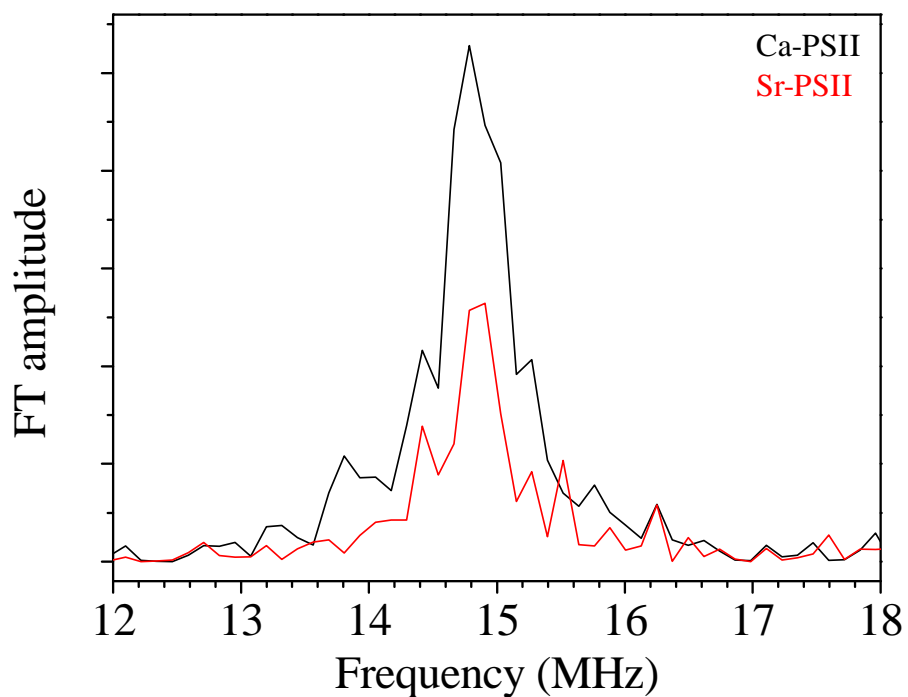
Figure S4:

Sequence of the amplitude of the absorption changes at 292 nm (black) and 440-426 nm (red) in WT* Sr-PSII. The measurements were done during a series of saturating flashes (spaced 400 ms apart). The samples (Chl = 25µg/ml) were dark-adapted for 1 h at 19°C before the addition of 100 µM PPBQ dissolved in DMSO. The measurements were done 200 ms after each flash.
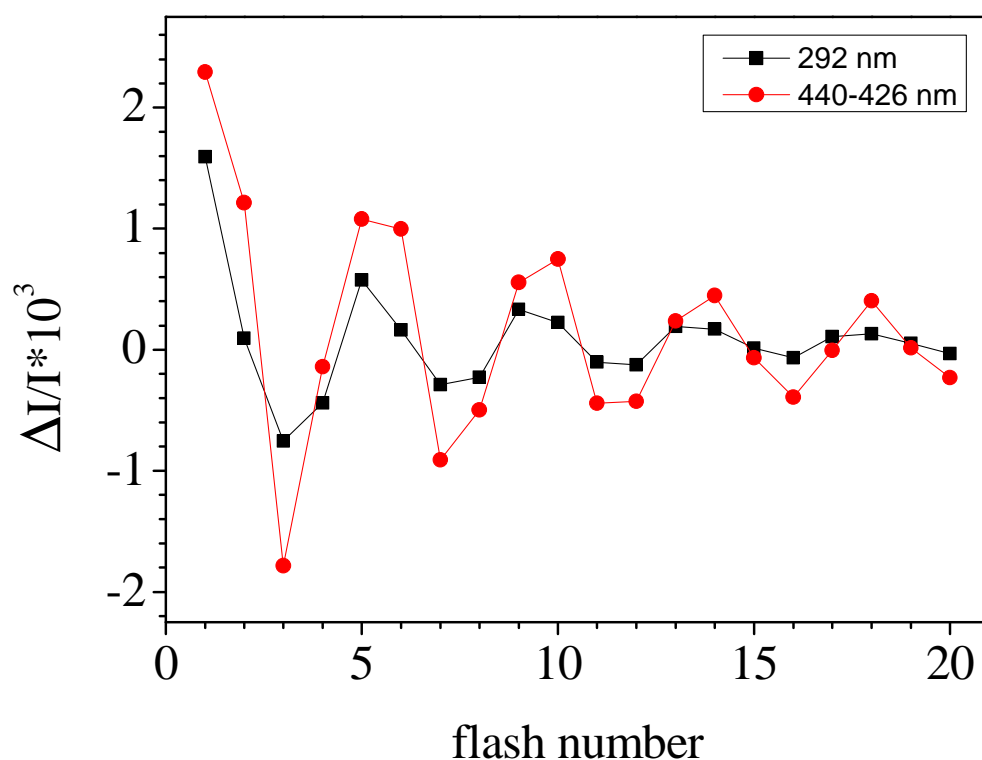
Figure S5:

Sequence of the amplitude of the absorption changes at 292 nm in WT* Sr-PSII at 5°C (black), 19°C (red) and 40°C (blue). The measurements were done during a series of saturating flashes (spaced 400 ms apart) given to WT* Sr-PSII. The samples (Chl = 25µg/ml) were dark-adapted for 1 h at 19°C before the addition of 100 µM PPBQ dissolved in DMSO. The measurements were done 200 ms after each flash.
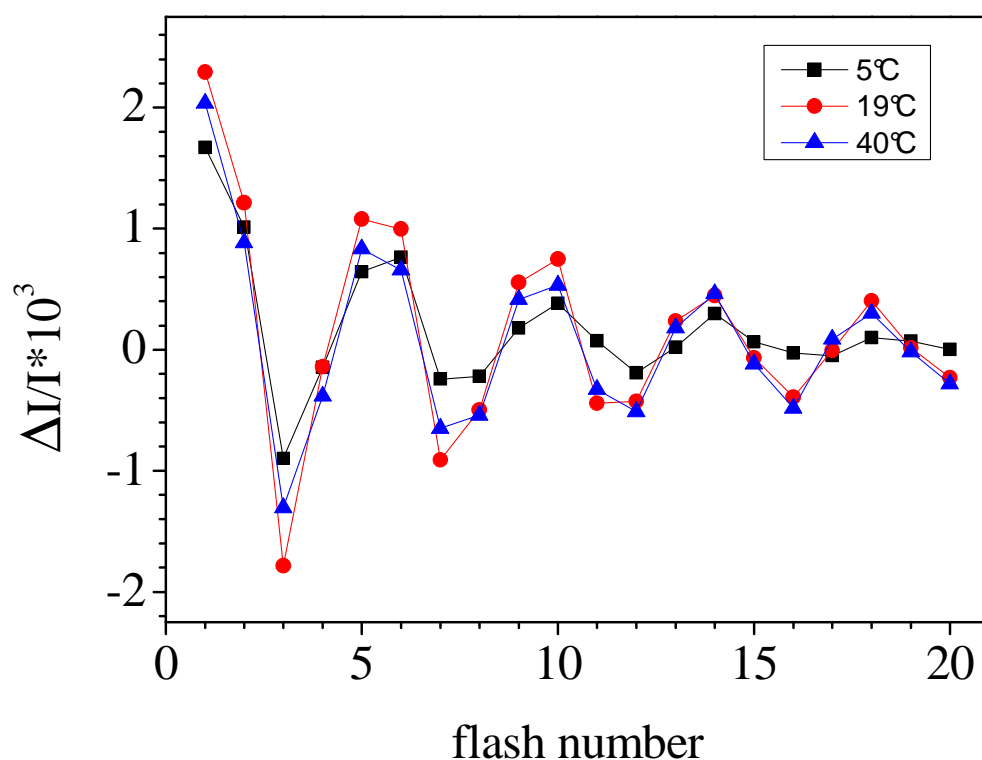
Figure S6:

Sequence of the amplitude of the absorption changes at 292 nm at 5°C in WT* Ca-PSII (black) and WT* Sr-PSII (red). The measurements were done during a series of saturating flashes (spaced 400 ms apart). The samples (Chl = 25µg/ml) were dark-adapted for 1 h at 19°C before the addition of 100 µM PPBQ dissolved in DMSO. The measurements were done 200 ms after each flash.